

Magnetite Particles Triggering a Faster and More Robust Syntrophic Pathway of Methanogenic Propionate Degradation

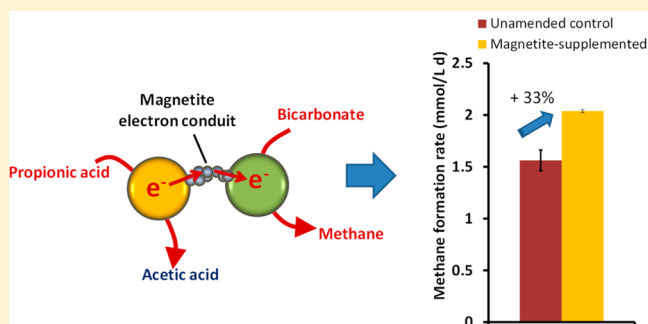
Carolina Cruz Viggli,[†] Simona Rossetti,[†] Stefano Fazi,[†] Paola Paiano,[†] Mauro Majone,[‡] and Federico Aulenta^{*,†}

[†]Water Research Institute (IRSA), National Research Council (CNR), via Salaria km 29.300, 00015 Monterotondo (RM), Italy

[‡]Department of Chemistry, Sapienza University of Rome, Piazzale Aldo Moro 5, 00185 Rome, Italy

S Supporting Information

ABSTRACT: Interspecies electron transfer mechanisms between *Bacteria* and *Archaea* play a pivotal role during methanogenic degradation of organic matter in natural and engineered anaerobic ecosystems. Growing evidence suggests that in syntrophic communities electron transfer does not rely exclusively on the exchange of diffusible molecules and energy carriers such as hydrogen or formate, rather microorganisms have the capability to exchange metabolic electrons in a more direct manner. Here, we show that supplementation of micrometer-size magnetite (Fe_3O_4) particles to a methanogenic sludge enhanced (up to 33%) the methane production rate from propionate, a key intermediate in the anaerobic digestion of organic matter and a model substrate to study energy-limited syntrophic communities. The stimulatory effect most probably resulted from the establishment of a direct interspecies electron transfer (DIET), based on magnetite particles serving as electron conduits between propionate-oxidizing acetogens and carbon dioxide-reducing methanogens. Theoretical calculations revealed that DIET allows electrons to be transferred among syntrophic partners at rates which are substantially higher than those attainable via interspecies H_2 transfer. Besides the remarkable potential for improving anaerobic digestion, which is a proven biological strategy for renewable energy production, the herein described conduction-based DIET could also have a role in natural methane emissions from magnetite-rich soils and sediments.



INTRODUCTION

Propionate is a central metabolite in the anaerobic degradation of organic matter and also a model substrate to study syntrophic relationships in energy-limited methanogenic ecosystems, in either natural environments such as freshwater sediments or engineered systems such as anaerobic bioreactors.^{1–3} Complete degradation of propionate to methane gas and carbon dioxide requires the concerted action of *Bacteria* and *Archaea*. Typically, acetogenic *Bacteria* oxidize propionate into acetic acid and H_2 (or formate),⁴ according to the following reaction: $\text{CH}_3\text{CH}_2\text{COO}^- + 3\text{H}_2\text{O} \rightarrow \text{CH}_3\text{COO}^- + \text{HCO}_3^- + \text{H}^+ + 3\text{H}_2$. Under standard biochemical conditions (i.e., substrates and products at 1 M or 1 atm, pH 7, and 298 K), this reaction is, however, energetically unfavorable ($\Delta G^{\circ'} = +76.0$ kJ/mol) and therefore is only possible (i.e., $\Delta G' < 0$) if the products, acetate and particularly H_2 , are kept at low concentration levels by the scavenging activity of acetoclastic and hydrogenophilic methanogenic *Archaea*. Interspecies H_2 (or formate) transfer between H_2 -producing acetogenic *Bacteria* and H_2 -consuming methanogenic *Archaea* has been for a long time assumed as the exclusive strategy underpinning syntrophic propionate degradation.^{5,6} Recent findings, however, have pinpointed the possibility that other interspecies energy transfer mechanisms, not relying on the exchange of diffusible

molecules or energy carriers among partners, may also play a role in syntrophic communities of anaerobic microorganisms.^{7–9} As an example, a study reported that an ethanol-fed, coculture of *Geobacter metallireducens* and *Geobacter sulfurreducens* formed electrically conductive aggregates whereby electrons released by *G. metallireducens* during ethanol oxidation were passed directly to *G. sulfurreducens* (for the reduction of fumarate to succinate) likely via conductive appendages (e.g., pili) and/or redox proteins (e.g., cytochromes).^{10,11} More recently, *G. metallireducens* was found to make direct electrical connections also with methanogenic organisms such as *Methanosaeta* species, with the latter organism accepting electrons via direct interspecies electron transfer (DIET) for carbon dioxide reduction to methane.¹² Further studies revealed that DIET could be sustained and stimulated by the addition of electrically conductive materials, such as activated carbon,¹³ and minerals such as magnetite,^{14–17} of nanometer to micrometer size, possibly serving as conduits

Received: April 4, 2014

Revised: June 5, 2014

Accepted: June 5, 2014

Published: June 5, 2014

between the electron-donating and the electron accepting organisms.

Here, we demonstrated that supply of magnetite particles is a viable strategy to trigger DIET in a methanogenic sludge and accordingly promote a route of propionate conversion into methane that is faster and less sensitive on external H_2 partial pressure than the “classical” one based on interspecies H_2 transfer. The experimental findings herein presented were corroborated by theoretical calculations suggesting that magnetite-mediated DIET is an intrinsically faster electron transfer mechanism compared to interspecies H_2 transfer.

MATERIALS AND METHODS

Synthesis of Magnetite Particles. Magnetite particles were synthesized according to a previously described protocol.¹⁸ Briefly, $FeCl_3$ (5.2 g) and $FeCl_2$ (2.0 g) were dissolved into an acidic (HCl 0.4 N) aqueous solution which was then added dropwise into a 1.5 N NaOH solution under vigorous mixing, generating an instant black precipitate of Fe_3O_4 (magnetite). The precipitate was isolated in the magnetic field, purified by centrifugation, and suspended in 0.25 L of deoxygenated water. The average diameters of synthesized magnetite particles were 100–150 nm.¹⁷ Dried precipitates were characterized by X-ray diffraction using a Rigaku D-max diffractometer, with a Cu $K\alpha$ radiation source. The obtained XRD pattern was compared to that of pure magnetite (Figure S1, Supporting Information).

Source Culture. The anaerobic methanogenic culture used as inoculum for batch experiments was collected from a mesophilic (37 °C) pilot-scale anaerobic digester operated in semicontinuous mode and fed with waste activated sludge, sampled from the municipal wastewater treatment plant of the city of Rome (Italy).

Batch Experiments. All batch experiments were conducted in anaerobic 120 mL serum bottles incubated statically, in the dark, at room temperature (20–25 °C). Bottles contained 57 mL of mineral medium, 1 mL of sodium bicarbonate (10 wt %/wt), and either 2 mL of a suspension of magnetite particles, corresponding to a final concentration of 0.35 g Fe/L (magnetite-amended bottles), or 2 mL of deionized water (unamended controls). The medium contained the following components: NH_4Cl (0.5 g/L), $MgCl_2 \cdot 6H_2O$ (0.1 g/L), K_2HPO_4 (0.4 g/L), and $CaCl_2 \cdot 2H_2O$ (0.05 g/L). Upon preparation, all bottles were sealed with Teflon-faced butyl rubber stoppers, flushed with a 70% N_2 /30% CO_2 gas mixture, inoculated with 1 mL of source culture [corresponding to an initial volatile suspended solids (VSS) concentration of 0.20 g/L] and spiked with propionate to a final concentration of approximately 6.5 mmol/L. The resulting initial specific magnetite load was 1.75 g Fe/gVSS. Throughout all incubations, the pH remained in the range of 7.5–7.8.

Once all the bottles had completely converted the initial dose of propionate (1st feeding cycle) into methane, they were flushed with the N_2/CO_2 gas mixture in order to remove the methane produced and then respiked with the substrate (2nd feeding cycle). During each feeding cycle, the bottles were sampled for the determination of propionate (and organic acids deriving from its degradation) and methane concentrations. At the end of each feeding cycle, the liquid volume removed for analysis was replaced with fresh anaerobic medium. Each experiment was performed in duplicate, and average values were reported. Additional batch experiments were also conducted whereby H_2 was added to the headspace of the

bottles in the presence and in the absence of propionate. The aim of these experiments was to assess the impact of H_2 on the kinetics and pathway of propionate degradation or to determine the maximum methanogenic hydrogenophilic activity of the biomass. Control bottles, prepared as above but incubated in the absence of propionate (both in the presence and in the absence of magnetite particles), were also set up in order to assess the impact of magnetite particles on the endogenous metabolism of the biomass.

Analytical Methods. Organic acids (acetate, propionate, butyrate, and isobutyrate) were analyzed by injecting 1 μL of filtered (0.22 μm porosity) liquid sample into a PerkinElmer Auto System gas chromatograph (2 m \times 2 mm stainless steel column packed with 60/80 mesh Carbopak B-DA 80–120 4% CW 20 M Supelco; N_2 carrier gas 20 mL/min; oven temperature 175 °C; injector temperature 200 °C; flame ionization detector (FID) temperature 250 °C). Methane was analyzed by injecting 10 μL of headspace sample (with a gastight Hamilton syringe) into a PerkinElmer GC 8500 gas chromatograph (2 m \times 2 mm stainless steel column packed with 60/80 mesh Carbopak B/1% SP-1000 Supelco; N_2 carrier gas 20 mL/min; oven temperature 190 °C; injector temperature 250 °C; FID temperature 250 °C). Methane production was referred to 25 °C and 1 bar.

Molecular and Microscopy Analysis of the Microbial Communities. Fluorescence in situ hybridization (FISH) analysis was performed on paraformaldehyde-fixed samples according to a procedure described elsewhere.^{19,20} Oligonucleotide probes specific for *Bacteria* (EUB338mix probes) and *Archaea* (ARC915 probe) domains were used. Details of the employed oligonucleotide probes are available at probeBase.²¹ In addition, FISH probes targeting *Methanosaetaceae* (MX825a,b,c) were applied in a mixture as reported elsewhere.²² Samples were examined by epifluorescence microscopy (Olympus BX51). All the hybridizations with specific probes were carried out in combination with DAPI staining to estimate the portion of cells targeted by group specific probes out of the total cells. Data were based on 10 fields of view per sample, with each sample analyzed in duplicate. The average number of DAPI-stained cells, per field of view, was in the range of 80–100.

In order to visualize specific cells within the 3D structure of the aggregates, FISH was combined with confocal laser scanning microscopy (CSLM; Olympus FV1000).^{23,24} The hybridized bacterial cells were excited with the 488 nm line of an Ar laser (excitation) and observed in the green channel from 500 to 530 nm (emission). *Archaea* cells were excited with the 543 nm line of a He–Ne laser and observed in the red channel from 550 to 660 nm. Magnetite particles were visualized by their reflection signal (405 nm line of a diode laser). The three-dimensional reconstruction of CSLM images was elaborated by the software IMARIS 7.6 (Bitplane, Switzerland).

RESULTS AND DISCUSSION

Influence of Magnetite Particles on the Kinetics of Methanogenic Propionate Degradation. In order to proceed at appreciable rates, propionate degradation under methanogenic conditions requires the establishment of a syntrophic cooperation between acetogenic *Bacteria*, typically converting propionate into acetate and H_2 (or other electron sinks such as formate), and methanogenic *Archaea* ultimately converting these compounds into methane gas. Here, in order to assess the influence of magnetite particles on the kinetics of

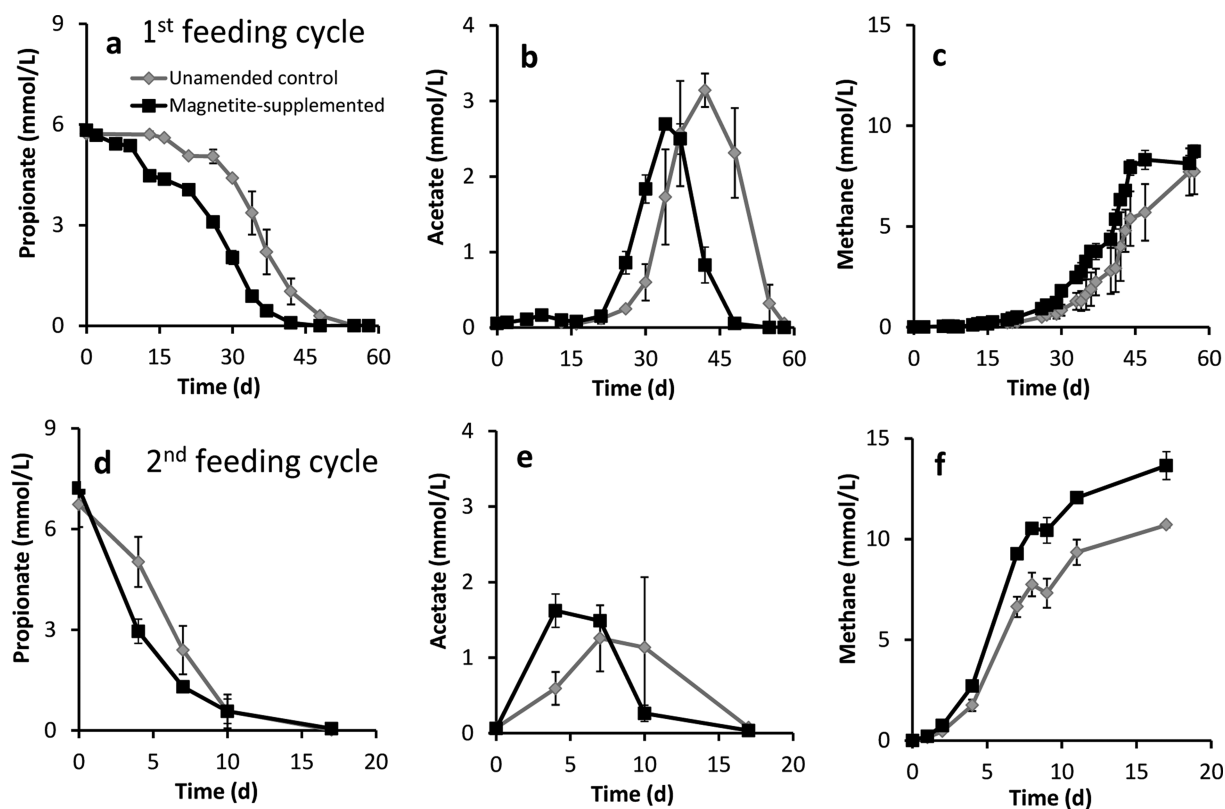


Figure 1. Time course of propionate (a,d), acetate (b,e), and methane (c,f) concentration in magnetite-supplemented bottles and unamended controls, in two successive feeding cycles. Error bars represent the standard deviation of replicate experiments.

propionate degradation to methane, a series of batch tests were conducted using an unacclimated methanogenic sludge as inoculum. In the first feeding cycle (Figure 1a–c), propionate degradation in bottles containing magnetite particles started after a slightly shorter lag phase (6 days vs 16 days) and proceeded to completion more rapidly (48 days vs 55 days) compared to unamended control bottles. Apparently, the pathway of propionate degradation was not substantially affected by the presence of magnetite since in both magnetite-supplemented bottles and unamended controls acetate was the only soluble intermediate detected during propionate degradation to methane. In magnetite-supplemented bottles, however, acetate reached a peak concentration earlier (day 34 vs day 42; indicative of a faster production from propionate) and was depleted sooner (day 55 vs day 58; indicative of faster conversion into methane) than in the corresponding unamended controls. Accordingly, methane (derived from both aceticlastic and hydrogenophilic methanogenesis) increased more rapidly in the presence of conductive particles than in the unamended controls.

However, the amount of methane ultimately produced from propionate (around 1.4 mol of methane per mol of propionate consumed) was slightly lower than the value (i.e., 1.75 mol of methane per mol of propionate consumed) predicted from the stoichiometry of the classical methanogenic propionate degradation pathway ($4\text{CH}_3\text{CH}_2\text{COO}^- + 4\text{H}^+ + 2\text{H}_2\text{O} \rightarrow 7\text{CH}_4 + 5\text{CO}_2$). Besides the fraction of propionate diverted to biomass growth which is typically lower than 5%,²⁵ this finding is probably due to the presence of low amounts of alternative electron acceptors such as sulfate or nitrate in the methanogenic sludge used as inoculum, which consumed part of the supplied propionate via sulfate reduction or denitrifica-

tion during the initial 20–25 days of incubation. Indeed, during this period, around 15% of the supplied propionate was removed without concomitant formation of acetic acid or methane.

During the second feeding cycle (Figure 1d–f), propionate degradation proceeded at a higher rate and did not display any initial lag phase, regardless the presence of magnetite particles. Compared to the previous cycle, acetate accumulated at lower concentrations and a higher amount of methane was ultimately produced, accounting for the stoichiometric conversion of the supplied propionate.

Figure 2a shows the maximum rate of methane formation calculated from the experiments reported in Figure 1 and from parallel control tests carried out, on the same inoculum, in the absence of propionate. For the experiments carried out in the presence of the substrate, the maximum rate of methane formation in magnetite amended bottles was always higher (33% higher in the first feeding cycle and 31% higher in the second feeding cycle) than in the corresponding unamended controls (Figure 2b). Apparently, the stimulatory effect of magnetite was substrate dependent since in tests lacking propionate the rate of “endogenous” methane formation was even higher (approximately 20%) in the absence of magnetite. This latter finding suggests that magnetite did not stimulate methanogenic activity by providing microorganisms involved in methanogenic propionate degradation with an additional source of electron donor or trace elements (e.g., iron ions) but rather facilitated the syntrophic conversion of the supplied substrate.

Influence of Magnetite Particles on Propionate Degradation Pathway at High H_2 Partial Pressure. Syntrophic interactions, including methanogenic propionate

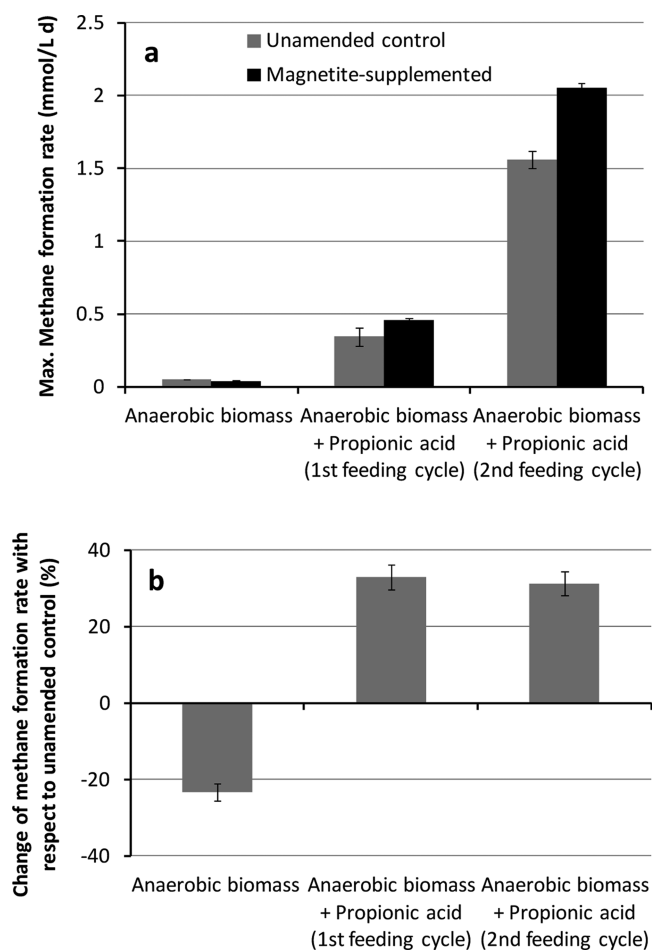


Figure 2. Maximum methane production rate (a) in magnetite-supplemented bottles and unamended controls. Relative change of methane production rate in magnetite-supplemented bottles with respect to unamended controls (b). Error bars represent the standard deviation of replicate experiments.

degradation, are usually associated with interspecies H_2 transfer. One key feature of these processes is that they are sustainable only if H_2 is maintained at low levels (typically below 10^{-5} atm) by the H_2 -scavenging activity of hydrogenophilic methanogens.²⁶ If this delicate balance between H_2 -producing and H_2 -consuming metabolisms is suddenly disrupted and H_2 accumulates, as sometimes it happens in methanogenic bioreactors following a substrate shock load, then propionate oxidation (to acetic acid and H_2) tends to slow down and/or proceed via alternative, energetically more favorable, degradation routes (e.g., propionate is dismutated to acetate and butyrate before being degraded via β -oxidation).⁴ Here, in order to verify the hypothesis that in the presence of magnetite the electron transfer may also proceed via electric conduction, hence through a pathway which does not involve an intermediate H_2 generation, batch experiments were carried out in which H_2 was spiked to the headspace of the bottles during propionate degradation (Figure 3).

When 0.08 mmol of H_2 (corresponding to a partial pressure of around 0.1 atm) was spiked to the headspace of the magnetite-supplemented bottles, propionate degradation started immediately and proceeded with apparent zero-order kinetics (Figure 3a). Clearly, since during propionate degradation the bottles were incubated statically, it is unlikely

that the H_2 in the headspace of the bottles was in equilibrium with that in the liquid phase. Accordingly, the actual H_2 concentration that microorganisms were exposed to was probably substantially lower than the value predicted by Henry's law. In unamended controls, propionate degradation rate was initially lower and increased over time, most probably as methanogens consumed H_2 and accordingly alleviated product inhibition effects.

The higher propionate degradation rate observed in magnetite-supplemented bottles was mirrored by a higher methane production rate (Figure 3d). It is worth noting that, unlike previously described experiments, butyrate, and to a lower extent isobutyrate, were also detected during propionate degradation (Figure 3c), testifying the onset of alternative propionate degradation pathways triggered by the presence of H_2 . In order to magnify the existing differences in terms of propionate degradation pathways between magnetite-supplemented bottles and unamended controls, all the bottles were respiked with propionate and a much higher amount of H_2 , corresponding to a partial pressure of 0.65 atm. Propionate was rapidly and completely degraded only in the presence of magnetite. Similarly, acetate was formed and consumed more rapidly; four carbon-atom acids remained at lower concentrations, and methane was produced in larger amounts and at a substantially higher rate. Overall, the propionate degradation rate and pathway in bottles containing magnetite was much less affected by the presence of H_2 than the unamended control. This finding provides an additional line of evidence that magnetite promoted the establishment of an interspecies electron route between acetogenic propionate oxidizers and methanogens not based on interspecies H_2 transfer. Considering, however, that, in the presence of externally added H_2 , butyrate and isobutyrate were formed (from propionate) also in the presence of magnetite (though at much lower concentration levels than in unamended controls), it is likely that, in magnetite supplemented cultures, the involved electron transfer mechanism was actually a hybrid of interspecies H_2 transfer and electrical conduction via magnetite particles.

Microbial Characterization. In syntrophic, propionate-fed cultures, the activity of propionate degraders is intimately dependent on the activity of methanogens and vice versa. Therefore, there is a possibility that the more robust methanogenic degradation of propionate, observed in magnetite-supplemented bottles, was ultimately due to the presence of a more abundant and/or active methanogenic population. To address this hypothesis, the relative abundance of *Bacteria* and *Archaea* (with these latter being representative of the methanogenic fraction of the biomass) in magnetite-supplemented bottles and unamended controls was carried out by FISH, on samples taken at the end of the kinetic tests. Notably, the percentage of *Archaea* with respect to the total cells, in magnetite-supplemented and in unamended controls (i.e., $37 \pm 2\%$ and $39 \pm 1\%$, respectively), was statistically indistinguishable (P -value = 0.33). In both cultures, *Bacteria* also accounted for approximately 40% of DAPI-stained cells (Table 1).

Visualization of the cultures using confocal laser scanning microscopy (CLSM) in combination with FISH revealed the presence of clustered biomass with *Archaea* always laying in close proximity to the *Bacteria* (Figure 4). Notably, the majority (>90%) of cells binding the oligonucleotide probe targeting *Archaea* appeared as rods mostly growing as long filaments, whereas a minor fraction of *Archaea* displayed a coccoidal morphology. The filamentous *Archaea* were further identified

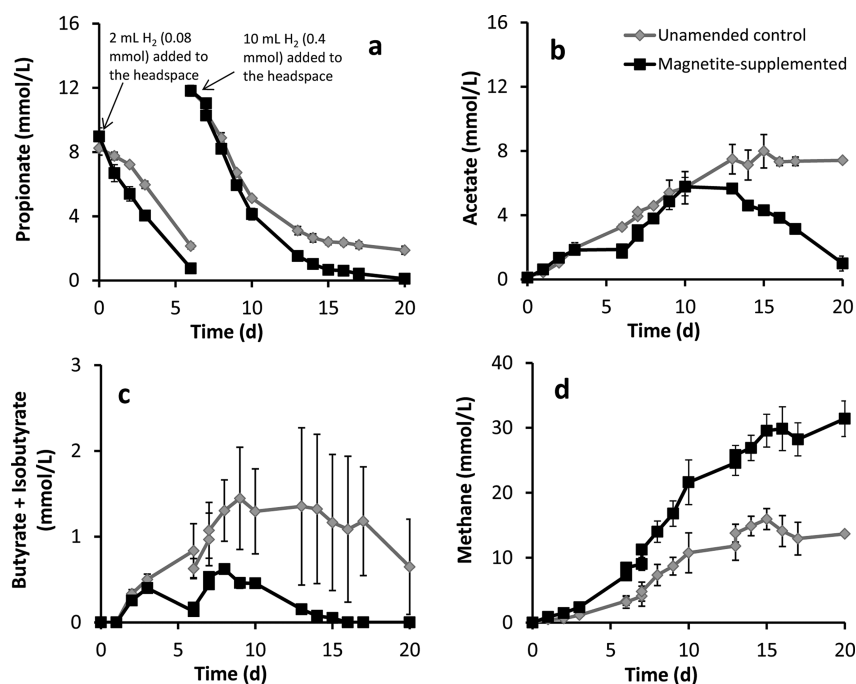


Figure 3. Time course of propionate (a), acetic acid (b), sum of butyrate and isobutyrate (c), and methane (d) concentration in magnetite-supplemented bottles and unamended controls, in propionate degradation batch tests conducted in the presence of (externally spiked) H_2 . Error bars represent the standard deviation of replicate experiments.

Table 1. Relative Amount of Bacteria and Archaea and Maximum Hydrogenophilic Methane Production Rate in Magnetite-Supplemented Cultures and Unamended Controls^a

	magnetite-supplemented culture	unamended control culture
bacteria/DAPI-stained cells (%)	38 ± 1	41 ± 1
Archaea/DAPI-stained cells (%)	37 ± 2	39 ± 1
max. hydrogenophilic methane formation rate (mmol CH_4/L d)	0.13 ± 0.02	0.14 ± 0.09

^aMean values ±1 standard deviation of replicate experiments.

by FISH as *Methanosaeta* species. This finding provides a strong additional line of evidence on the ability of *Methanosaeta* to generate methane not only from acetate cleavage but also from bicarbonate reduction, as recently reported,²⁷ with electrons taken up via magnetite-mediated DIET. Most probably, the remainder of *Archaea*, not binding with the *Methanosaeta* probes, was hydrogenophilic methanogens, thriving on the hydrogen released upon propionate oxidation. In syntrophic cultures, clustering is essential to minimize the diffusion distance of interspecies electron carriers between a producing (acetogen) and a consuming (methanogen) organism and accordingly to maximize the rate of substrate conversion. Here, the presence of aggregates of apparently similar shapes and composition (Figure S2, Supporting Information) in both the magnetite-supplemented cultures and the unamended controls indicates that magnetite particles did not affect propionate degradation by simply providing a solid surface for a more effective biomass attachment. In spite of that, however, magnetite particles were found to be closely associated with the microbial aggregates, pointing to their direct interaction with microbial cells and metabolism (Figure 4).

To obtain an additional independent estimate of the maximum hydrogenophilic (H_2 dependent) methanogenic activity of the magnetite-supplemented bottles and of the unamended controls, the maximum methane production rate was determined after flushing the headspace of the bottles with pure H_2 and after verifying that no residual propionate or other organic substrates were present in the bottles. Remarkably, the maximum methane production rate in the two cultures was essentially the same (Table 1). Taken as a whole, these findings strongly suggest that the observed effect of magnetite particles on the rate and pathway of propionate degradation cannot be explained in terms of differences in the hydrogenophilic methanogenic activity or of degree of biomass aggregation. Conversely, the improved methanogenic conversion of propionate evokes a faster and more robust electron transfer process between acetogens and methanogens. This electron transfer process, presumably additive to the one based on interspecies H_2 transfer, most probably involved the conduction of electrons through the magnetite particles, as schematically depicted in Figure 5.

In principle, the stimulatory effect of magnetite on propionate degradation and methane formation could also be due to the scavenging of hydrogen by magnetite, with the reaction being catalyzed by bacteria. Indeed, it has been shown that, under acidic conditions, magnetite can serve as terminal electron acceptor in the energy metabolism of dissimilatory iron reducing bacteria.²⁸ However, thermodynamic calculations (Figure S3, Supporting Information) show that, at pH 7.6 (the average pH during incubations reported in Figure 1), this reaction becomes energetically unfavorable when Fe(II) accumulates at extremely low (5×10^{-7} M) concentration levels. This demonstrates that, under the batch conditions of the herein described experiments, magnetite represents an insignificant sink of H_2 . On the other hand, under acidic conditions and/or in continuous-flow systems whereby Fe(II)

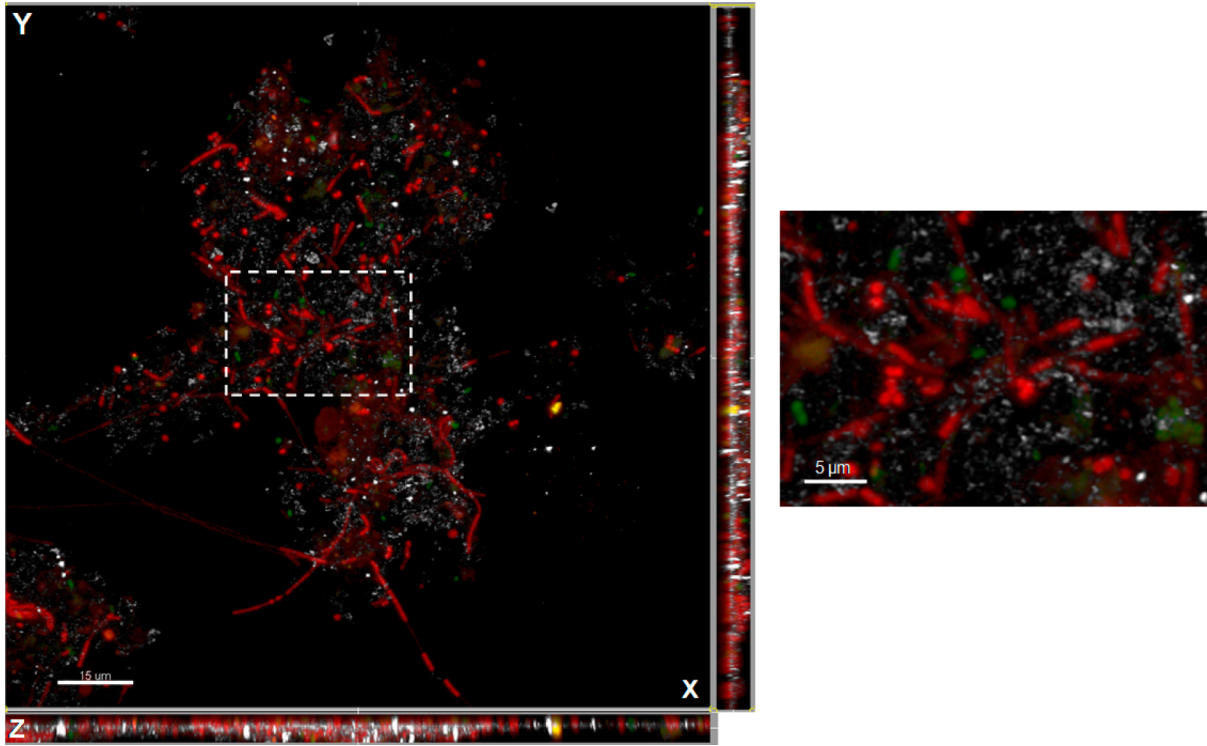


Figure 4. CLSM combined images showing the spatial distribution (X–Y, X–Z, and Y–Z planes) of *Archaea* (red) and *Bacteria* (green) cells identified by FISH in aggregates from the magnetite-supplemented cultures. Magnetite particles, visualized by their reflection signal in the same microscopic field, appear gray. A detail of the aggregate is reported on the right. The image is composed by 15 optical sections of the aggregate thickness every 0.45 μm.

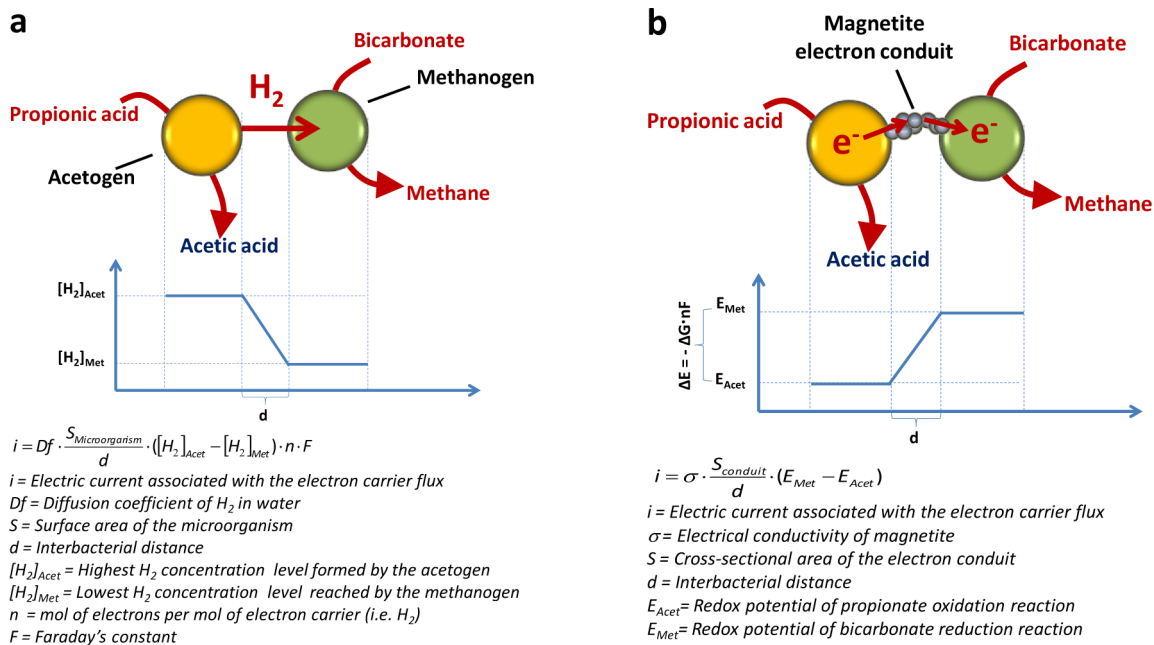


Figure 5. Proposed electron transfer mechanisms between an acetogen and a methanogen in magnetite supplemented cultures: interspecies H₂ transfer (A) and electronic conduction through magnetite particles (B). For each of the two mechanisms, a simplified model to compute the electric current associated with the flux of electron carriers (electrons or H₂) is also depicted.

accumulation can be minimized, this mechanism could also play a key role. This hypothesis, however, warrants further investigations.

Theoretical Analysis of Interspecies Electron Transfer via Electronic Conduction and via H₂ Diffusion. Figure 5 illustrates the proposed electron transfer mechanisms, from an

acetogen to a methanogen, which involve either diffusive H₂ exchange (a) or electric conduction through a magnetite-based conduit (b), without intermediate H₂ formation. In order to quantitatively compare the intrinsic kinetic efficiency of these two mechanisms, the corresponding maximum attainable electron carrier fluxes were calculated (Figure 5).

In the case of interspecies H_2 transfer, the electron carrier (i.e., H_2) flux was calculated using a previously reported approach,^{1,29,30} whereby Fick's law is used to compute the rate of H_2 diffusion from the acetogen to the methanogens. In this case, the maximum possible driving force for H_2 diffusion is given by the difference between the highest concentration of H_2 which can be generated by the acetogen during propionate oxidation (i.e., approximately 180 nM, corresponding to $\Delta G' = 0$) and the lowest H_2 concentration which can be reached by the methanogens (i.e., approximately 0.5 nM, corresponding to $\Delta G' = 0$) during bicarbonate reduction. To compute these thermodynamic values, the following concentrations for substrates and products were used: propionate 5×10^{-3} mol/L, acetate 5×10^{-4} mol/L, bicarbonate 3×10^{-2} mol/L, and methane 5×10^{-4} atm. To estimate the corresponding maximum H_2 flux, an interbacterial distance of 0.5 μm was assumed, with cells (both the acetogen and the methanogen) having an arbitrary spherical shape with an average diameter of 2 μm and a diffusion constant of H_2 in water of 4.5×10 cm^2/s .^{5,30} Under all these assumptions, the calculated maximum H_2 flux was approximately 2×10^{-8} nmol/s, which would theoretically correspond to an equivalent electric current of 4×10^{-12} A. In a similar way, the maximum electron carrier flux for the electronic conduction-based mechanism was calculated assuming that the electrons released upon propionate oxidation (according to the stoichiometry of the following half-reaction: $4\text{Propionate}^- + 12\text{H}_2\text{O} \rightarrow 4\text{Acetate}^- + 4\text{HCO}_3^- + 28\text{H}^+ + 24\text{e}^-$) are conveyed to a methanogen via an electron conduit consisting of aligned magnetite particles, with the microorganism using them to reduce bicarbonate to methane gas (according to the stoichiometry of the following half-reaction: $3\text{HCO}_3^- + 27\text{H}^+ + 24\text{e}^- \rightarrow 3\text{CH}_4 + 9\text{H}_2\text{O}$). The electron conduit was modeled as a wire having a diameter of 100 nm, recalling the average diameter of particles which was determined by scanning electron microscopy and flow cytometry analysis.¹⁷

Here, the maximum driving force for electron transfer is given by the redox potential (ΔE) of the overall reaction ($4\text{Propionate}^- + 3\text{H}_2\text{O} \rightarrow 4\text{Acetate}^- + \text{HCO}_3^- + \text{H}^+ + 3\text{CH}_4$) which accounted for approximately 0.070 V. To compute this value, the concentrations of reactants and products (as well as all other boundary conditions) were set identical to those used to calculate electron carrier flux in the case of H_2 transfer (i.e., propionate 5×10^{-3} mol/L; acetate 5×10^{-4} mol/L; bicarbonate 3×10^{-2} mol/L; methane 5×10^{-4} atm). The value used for the electrical conductivity of magnetite was 2.5×10^2 Ωcm^{-2} .³¹ The resulting maximum electron carrier flux via electrical conduction was in the order of 3×10^{-5} A, hence around 10^6 times higher than that associated with the interspecies H_2 transfer. Clearly, a number of assumptions was made to compute the electron carrier fluxes, some of which are certainly questionable. As an example, the assumption that the driving force for electron transfer is given by the Gibbs free energy of the reaction intrinsically implies that no energy is conserved by the microorganisms for growth and maintenance purposes and no energy is lost as heat, which is certainly not the case. Notwithstanding these considerations, the computed difference between the two fluxes is so large (i.e., a 10^6 factor) that the kinetic advantage arising from the interspecies electron transfer via electrical conduction is apparent.

In the present study, the addition of magnetite particles resulted, in each feeding cycle, in a relative increase of the methane formation rate of around 31–33%. Hence, the

maximum attained methane formation rate remained substantially lower than that predicted by interspecies electron transfer calculations. This suggests that, in the presence of magnetite, the “resistance” to methane formation associated with the interspecies electron transfer is virtually eliminated and methane formation becomes rate limited by the intrinsic activity of other (enzymatic) steps or overpotentials on the electron donating and/or electron accepting reactions.

Implications. Due to their unique physical–chemical properties, magnetic (nano)particles are being recently considered for an increasing number of applications, spanning from heterogeneous catalysis³² to drug delivery.^{33,34} The recent discovery that magnetite particles can promote DIET, and by so doing can alter the metabolism of syntrophic microbial communities, represents a new and virtually unexplored field of application for these electrically conductive materials, potentially relevant to industrial and environmental biotechnologies (i.e., from biofuels generation to bioremediation). Notably, the finding that, in the present study, the positive effect on methane generation resulting from the addition of magnetite particles could be verified on a “real” methanogenic sludge taken from a functioning anaerobic digester (not on “ad hoc” assembled cocultures) and on propionate, which is a central metabolite during the methanogenic degradation of the organic matter, pinpoints a factual potential to improve existing anaerobic digestion systems by promoting DIET, also in consideration of the fact that strategies to retain magnetite particles of micrometer-size in bioreactors are already available at commercial scale.

Specifically, the addition of magnetite particles may represent a novel, still unexplored, strategy to attenuate the impact of shock loads in anaerobic digestion systems, typically caused by sudden variations in the influent flow rate and substrate concentration, which often result in the accumulation of propionate and butyrate and ultimately in incomplete methanogenesis.³⁵ Taking into consideration that anaerobic digestion is one of the few proven renewable energy biotechnologies, with thousands full-scale plants worldwide, the results herein presented could have a broad impact. Finally, considering that magnetite is a ubiquitous mineral in anaerobic ecosystems, it is possible that magnetite-driven DIET could contribute significantly to natural methane emissions from magnetite-rich soils.

■ ASSOCIATED CONTENT

📄 Supporting Information

XRD diffraction (Figure S1) of synthesized particles; micrographs showing simultaneous visualization of magnetite particles, DAPI-stained cells, *Bacteria* and *Archaea* in samples taken from the magnetite-supplemented culture and unamended control (Figure S2); energetics of hydrogen oxidation by magnetite (Figure S3). This material is available free of charge via the Internet at <http://pubs.acs.org>.

■ AUTHOR INFORMATION

Corresponding Author

*E-mail: Aulenta@irsa.cnr.it; tel: +39 06 90672751; fax: +39 06 90672787.

Notes

The authors declare no competing financial interest.

ACKNOWLEDGMENTS

Josef Hossoun is greatly acknowledged for acquiring XRD spectra of magnetite particles. The authors thank the Advanced Centre for Microscopy "P. Albertano" of University of Rome "Tor Vergata" for CLSM analyses.

REFERENCES

- (1) de Bok, F. A. M.; Plugge, C. M.; Stams, A. J. M. Interspecies electron transfer in methanogenic propionate degrading consortia. *Water Res.* **2004**, *38* (6), 1368–1375.
- (2) Muller, N.; Worm, P.; Schink, B.; Stams, A. J. M.; Plugge, C. M. Syntrophic butyrate and propionate oxidation processes: From genomes to reaction mechanisms. *Environ. Microbiol. Rep.* **2010**, *2* (4), 489–499.
- (3) McCarty, P. L. The development of anaerobic treatment and its future. *Water Sci. Technol.* **2001**, *44* (8), 149–156.
- (4) Dolfing, J. Syntrophic propionate oxidation via butyrate: A novel window of opportunity under methanogenic conditions. *Appl. Environ. Microbiol.* **2013**, *79* (14), 4515–4516.
- (5) Stams, A. J. M.; de Bok, F. A. M.; Plugge, C. M.; van Eekert, M. H. A.; Dolfing, J.; Schraa, G. Exocellular electron transfer in anaerobic microbial communities. *Environ. Microbiol.* **2006**, *8* (3), 371–382.
- (6) Stams, A. J. M.; Plugge, C. M. Electron transfer in syntrophic communities of anaerobic bacteria and archaea. *Nat. Rev. Microbiol.* **2009**, *7* (8), 568–577.
- (7) Lovley, D. R. Live wires: Direct extracellular electron exchange for bioenergy and the bioremediation of energy-related contamination. *Energy Environ. Sci.* **2011**, *4* (12), 4896–4906.
- (8) Lovley, D. R. Reach out and touch someone: Potential impact of DIET (direct interspecies energy transfer) on anaerobic biogeochemistry, bioremediation, and bioenergy. *Rev. Environ. Sci. Bio/Technol.* **2011**, *10* (2), 101–105.
- (9) Malvankar, N. S.; Lovley, D. R. Microbial nanowires: A new paradigm for biological electron transfer and bioelectronics. *ChemSusChem* **2012**, *5* (6), 1039–1046.
- (10) Summers, Z. M.; Fogarty, H. E.; Leang, C.; Franks, A. E.; Malvankar, N. S.; Lovley, D. R. Direct exchange of electrons within aggregates of an evolved syntrophic coculture of anaerobic bacteria. *Science* **2010**, *330* (6009), 1413–1415.
- (11) Nagarajan, H.; Embree, M.; Rotaru, A. E.; Shrestha, P. M.; Feist, A. M.; Palsson, B.; Lovley, D. R.; Zengler, K. Characterization and modelling of interspecies electron transfer mechanisms and microbial community dynamics of a syntrophic association. *Nat. Commun.* **2013**, *4*, Article number: 2809; DOI:10.1038/ncomms3809.
- (12) Rotaru, A. E.; Shrestha, P. M.; Liu, F.; Shrestha, M.; Shrestha, D.; Embree, M.; Zengler, K.; Wardman, C.; Nevin, K.; Lovley, D. A new model for electron flow during anaerobic digestion: Direct interspecies electron transfer to Methanosaeta for the reduction of carbon dioxide to methane. *Energy Environ. Sci.* **2014**, *7*, 408–415.
- (13) Liu, F. H.; Rotaru, A. E.; Shrestha, P. M.; Malvankar, N. S.; Nevin, K. P.; Lovley, D. R. Promoting direct interspecies electron transfer with activated carbon. *Energy Environ. Sci.* **2012**, *5* (10), 8982–8989.
- (14) Kato, S.; Hashimoto, K.; Watanabe, K. Methanogenesis facilitated by electric syntrophy via (semi)conductive iron-oxide minerals. *Environ. Microbiol.* **2012**, *14* (7), 1646–1654.
- (15) Kato, S.; Hashimoto, K.; Watanabe, K. Microbial interspecies electron transfer via electric currents through conductive minerals. *Proc. Natl. Acad. Sci. U.S.A.* **2012**, *109* (25), 10042–10046.
- (16) Kato, S.; Nakamura, R.; Kai, F.; Watanabe, K.; Hashimoto, K. Respiratory interactions of soil bacteria with (semi)conductive iron-oxide minerals. *Environ. Microbiol.* **2010**, *12* (12), 3114–3123.
- (17) Aulenta, F.; Rossetti, S.; Amalfitano, S.; Majone, M.; Tandoi, V. Conductive magnetite nanoparticles accelerate the microbial reductive dechlorination of trichloroethene by promoting interspecies electron transfer processes. *ChemSusChem* **2013**, *6* (3), 433–436.
- (18) Kang, Y. S.; Risbud, S.; Rabolt, J. F.; Stroeve, P. Synthesis and characterization of nanometer-size Fe₃O₄ and gamma-Fe₂O₃ particles. *Chem. Mater.* **1996**, *8* (9), 2209–2211.
- (19) Rossetti, S.; Aulenta, F.; Majone, M.; Crocetti, G.; Tandoi, V. Structure analysis and performance of a microbial community from a contaminated aquifer involved in the complete reductive dechlorination of 1,1,2,2-tetrachloroethane to ethene. *Biotechnol. Bioeng.* **2008**, *100* (2), 240–249.
- (20) Amann, R. I.; Ludwig, W.; Schleifer, K. H. Phylogenetic identification and in-situ detection of individual microbial-cells without cultivation. *Microbiol. Rev.* **1995**, *59* (1), 143–169.
- (21) Loy, A.; Horn, M.; Wagner, M. probeBase: An online resource for rRNA-targeted oligonucleotide probes. *Nucleic Acids Res.* **2003**, *31* (1), 514–516.
- (22) Crocetti, G.; Murto, M.; Bjornsson, L. An update and optimization of oligonucleotide probes targeting methanogenic Archaea for use in fluorescence in situ hybridisation (FISH). *J. Microbiol. Methods* **2006**, *65* (1), 194–201.
- (23) Amann, R.; Lemmer, H.; Wagner, M. Monitoring the community structure of wastewater treatment plants: A comparison of old and new techniques. *FEMS Microbiol. Ecol.* **1998**, *25* (3), 205–215.
- (24) Lupini, G.; Proia, L.; Di Maio, M.; Amalfitano, S.; Fazi, S. CARD-FISH and confocal laser scanner microscopy to assess successional changes of the bacterial community in freshwater biofilms. *J. Microbiol. Methods* **2011**, *86* (2), 248–251.
- (25) Siegrist, H.; Vogt, D.; Garcia-Heras, J. L.; Gujer, W. Mathematical model for meso- and thermophilic anaerobic sewage sludge digestion. *Environ. Sci. Technol.* **2002**, *36* (5), 1113–1123.
- (26) Schmidt, J. E.; Ahring, B. K. Interspecies electron-transfer during propionate and butyrate degradation in mesophilic, granular sludge. *Appl. Environ. Microbiol.* **1995**, *61* (7), 2765–2767.
- (27) Rotaru, A. E.; Shrestha, P. M.; Liu, F.; Shrestha, M.; Shrestha, D.; Embree, M.; Zengler, K.; Wardman, C.; Nevin, K.; Lovley, D. A new model for electron flow during anaerobic digestion: Direct interspecies electron transfer to Methanosaeta for the reduction of carbon dioxide to methane. *Energy Environ. Sci.* **2013**.
- (28) Kostka, J. E.; Nealson, K. H. Dissolution and reduction of magnetite by bacteria. *Environ. Sci. Technol.* **1995**, *29* (10), 2535–2540.
- (29) Felchner-Zwirolo, M.; Winter, J.; Gallert, C. Interspecies distances between propionic acid degraders and methanogens in syntrophic consortia for optimal hydrogen transfer. *Appl. Microbiol. Biotechnol.* **2013**, *97* (20), 9193–9205.
- (30) Dong, X. Z.; Stams, A. J. M. Evidence for H₂ and formate formation during syntrophic butyrate and propionate degradation. *Anaerobe* **1995**, *1* (1), 35–39.
- (31) Verwey, E. J. W. Electronic conduction of magnetite (Fe₃O₄) and its transition point at low temperatures. *Nature* **1939**, *144*, 327–328.
- (32) Galvis, H. M. T.; Bitter, J. H.; Khare, C. B.; Ruitenbeek, M.; Dugulan, A. I.; de Jong, K. P. Supported iron nanoparticles as catalysts for sustainable production of lower olefins. *Science* **2012**, *335* (6070), 835–838.
- (33) Colombo, M.; Carregal-Romero, S.; Casula, M. F.; Gutierrez, L.; Morales, M. P.; Bohm, I. B.; Heverhagen, J. T.; Prospero, D.; Parak, W. J. Biological applications of magnetic nanoparticles. *Chem. Soc. Rev.* **2012**, *41* (11), 4306–4334.
- (34) Cheng, Z. L.; Al Zaki, A.; Hui, J. Z.; Muzykantov, V. R.; Tsourkas, A. Multifunctional nanoparticles: Cost versus benefit of adding targeting and imaging capabilities. *Science* **2012**, *338* (6109), 903–910.
- (35) Leitao, R. C.; Santaella, S. T.; van Haandel, A. C.; Zeeman, G.; Lettinga, G. The effects of hydraulic and organic shock loads on the robustness of upflow anaerobic sludge blanket reactors treating sewage. *Water Sci. Technol.* **2006**, *54*, 49–55.